

HYDROFOIL ROUGHNESS EFFECTS ON VON KÁRMÁN VORTEX SHEDDING

Philippe AUSONI *

Laboratory for Hydraulic Machines,
Ecole Polytechnique Fédérale de Lausanne

Mohamed FARHAT

Laboratory for Hydraulic Machines,
Ecole Polytechnique Fédérale de Lausanne

François AVELLAN

Laboratory for Hydraulic Machines,
Ecole Polytechnique Fédérale de Lausanne

*Corresponding author: Avenue Cour 33bis, CH-1007 Lausanne, Switzerland
Tel.: +41216934278, Fax: +41216933554, E-mail: philippe.ausoni@epfl.ch

ABSTRACT

The shedding process of the von Kármán vortices is shown to be highly related to the state of the boundary layer over the entire hydrofoil: The selected hydrofoil has a laminar-turbulent boundary layer transition at mid-chord for an incidence angle of 0° and tested Reynolds number range. With the help of a distributed roughness, the transition to turbulence is triggered at leading edge. The vortex shedding frequency and the vortex-induced vibration are compared for the two roughness configurations. Cavitation is used as a mean of visualization of the wake flow: Since vortex-induced vibration and high speed visualization are synchronized, the hydrofoil vibration level is considered versus the vortex span-wise organization. The occurrence of the 3D structures of shed vortices and the modulation of the vortex-induced vibration signals are investigated.

1. INTRODUCTION

Many authors observe that the wake structure may exhibit three-dimensional (3D) aspects even if the obstacle and the upcoming flow are 2D, see Williamson¹ for a review on the 3D structures of shed vortices. Williamson² describes the natural and forced formation of vortex dislocation in the cylinder wake and presents similarities of dislocation with boundary-layer spots. In many applications, the flow fields in which bodies are immersed are turbulent and the 3D aspects of the wake arise not only from end conditions but also from the turbulence of the shear layers and the wake, Szepessy³. It is known that the introduction of turbulence to the flow field promotes the vortex shedding critical transition at lower Reynolds numbers than it is the case in laminar flows. Moreover, increas-

ing the surface roughness of the body has a similar effect, Achenbach and Heinecke⁴. At higher Reynolds number, it is shown that the vortex shedding frequency is drastically decreased for rough cylinders in comparison with very smooth surface⁴. Wind-tunnel study shows that the introduction of free-stream turbulence acted to increase cylinder lift coefficients above those for laminar flow, Cheung and Melbourne⁵. Blackburn and Melbourne⁶ examine the effects of grid-generated turbulence on lift forces at sections of a circular cylinder. According to spectra and correlation length analysis, it is thought that the increase of the turbulence intensity of the mean flow promotes the re-establishment of organized vortex shedding. Ausoni *et al.*⁷ evaluate the ability of an unsteady numerical simulation to accurately reproduce the hydrofoil vortex shedding frequency and reveal that differences in the boundary layer transition point between experiments and computations have to be minimized in order to get good agreement

When the pressure is low enough, cavitation develops in the vortices cores. Young and Holl⁸ investigate the case of a flow around wedges and observe that the cavitation development in the wake increases the vortex shedding frequency by up to 25% and therefore affects the dynamic of the von Kármán street. Ausoni *et al.*⁹ confirms these results in the case of a 2D hydrofoil and investigate the influence of cavitation on vortex dislocations: Comparison of instantaneous velocity fields in cavitation free regime and high speed visualization of vortices cavitation does not show notable influence of the cavitation on the vortex street pattern. In terms of vortex spanwise organization, cavitation can therefore be considered as a passive agent of wake structure visualization. Moreover, Ausoni *et al.*¹⁰ investigate the cavitation

influence on von Kármán vortex shedding and induced hydrofoil vibrations. For the wake cavitation inception index, a new correlation relationship is proposed and validated: In contrast to the earlier models, the new correlation takes into account the trailing edge displacement velocity for lock-in condition. In addition, it is found that the transverse velocity of the trailing edge increases the vortex strength linearly.

2. EXPERIMENTAL SETUP

The EPFL high-speed cavitation tunnel is a closed loop with a test section of 150x150x750 mm, Avellan *et al.*¹¹. The operating flow parameters are the reference velocity at the test section inlet C_{ref} , the hydrofoil incidence angle α and the cavitation index $\sigma = 2(p_{inlet} - p_v) / \rho C_{ref}^2$ where p_{inlet} and p_v are respectively the reference pressure at the test section inlet and the vapor pressure. For all the presented results, the incidence angle of the hydrofoil α is fixed at 0° .

The experimental 2D hydrofoil, sketched in Figure 1, is a blunt truncated Naca0009 made of stainless steel. The trailing edge thickness h is 3.22 mm and its chord length L and span b are 100 mm and 150 mm respectively.

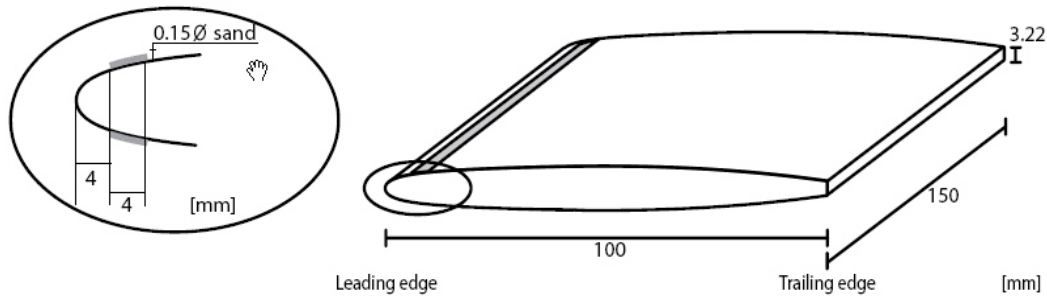


Figure 1. Blunt truncated Naca0009 hydrofoil and distributed roughness

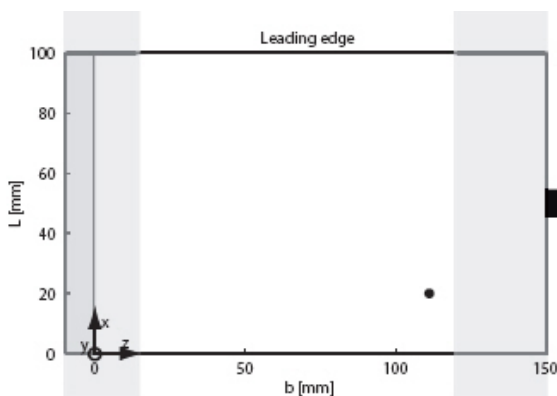


Figure 2 : Location of the hydrofoil vibration amplitude measurements point

A laser vibrometer is used to monitor the hydrofoil vortex-induced vibration. The measurement principle of this non-intrusive device is based on the detection of the frequency shift of the reflected laser beam, which is directly related to the displacement velocity of the surface in the laser direction according to the Doppler effect. The location of the measure-

ments points is shown in Figure 2. The data acquisition system has 16 bits A/D resolution, 16 inputs, a memory depth of 1 MSamples/Channel and a maximum sampling frequency of 51.2 kHz/Channel. The cavitation vortical structures in the hydrofoil wake are visualized with the help of a high speed digital camera. The CCD image resolution is 512x256 pixels at 10'000 frames/sec.

With the help of wall pressure measurements, Caron¹² evidences that the natural boundary layer transition to turbulence for this hydrofoil is located slightly downstream of the mid-chord for an incidence angle of 0° and Reynolds number $Re_h = C_{ref}h/\nu$ between $42 \cdot 10^3$ and $70 \cdot 10^3$. Ait Bouziad¹³ reports boundary layer computations and evaluates its thickness downstream from leading edge, $\delta \sim 100 \mu\text{m}$. In order to investigate the wall roughness effects on the vortex shedding process, a distributed roughness made of glue and 125 μm diameter sand is placed on both sides of the hydrofoil, 4 mm downstream to stagnation line and 4 mm wide, Figure 1. The glue and sand combination makes a two-dimensional flow obstacle of 150 μm height. Dryden¹⁴ reviews published data on the effect of roughness on transition from laminar to turbulent flow and shows that, for incompressible flow, the transition occurs when $C_{ref}k/\nu \geq 900$ where k is the height of the surface roughness pattern. Considering this relation in our case study, the triggered boundary layer transition occurs from 6 m/s upstream velocity. In the rest of the article, this configuration will be designated *rough*. In contrast, the case without rough strips will be designated *smooth*.

ments points is shown in Figure 2. The data acquisition system has 16 bits A/D resolution, 16 inputs, a memory depth of 1 MSamples/Channel and a maximum sampling frequency of 51.2 kHz/Channel. The cavitation vortical structures in the hydrofoil wake are visualized with the help of a high speed digital camera. The CCD image resolution is 512x256 pixels at 10'000 frames/sec.

3. RESULTS

A. Kármán shedding frequency

The vortex shedding frequency f_s , obtained from the vibration signals, is plotted in Figure 3 as a function of the flow velocity for the two roughness configurations. A linear relationship between the vortex shedding frequency and the upstream velocity is observed, the generation process of von Kármán vortices occurring at constant Strouhal number, $St = f_s h / C_{ref}$. It is found that the vortex shedding frequency is significantly decreased for the rough configuration. The mean Strouhal number value decreases from 0.24 for

the smooth leading edge to 0.18 for the rough one. As mentioned earlier, the natural boundary layer transition to turbulence is located at the hydrofoil mid-chord. With the rough leading edge, the turbulent boundary layer is triggered at leading edge. Since the turbulent boundary layer grows thicker than laminar one, it results that the trailing edge wake thickness of the rough configuration is larger than the one with smooth leading edge. Admitting a constant Strouhal number based on the wake thickness, the vortex shedding frequency varies inversely with this thickness and explains the decrease of the shedding frequency with the roughness.

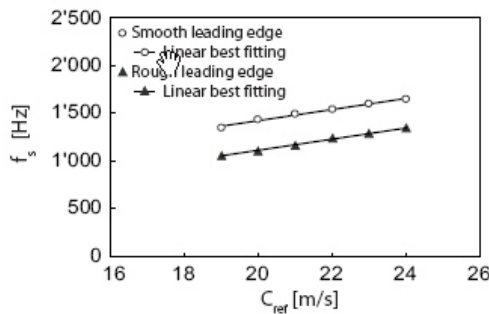


Figure 3. Shedding frequency of von Kármán vortices for different upstream velocities and roughness configurations, cavitation free

B. Wake structures and induced vibrations

Synchronized wake high speed visualizations and vortex-induced hydrofoil vibration measurements are evidenced in Figure 4. For the smooth leading edge, Figure 4 left, the vibration signals exhibit intermittent weak shedding cycles, which are typical of the occurrence of vortex dislocations, Szepessy *et al.*¹⁵. Indeed, a direct relationship is observed between the vortices span-wise organization and the vortex-induced vibration level: For parallel vortex shedding, the fluctuating force on the body is maximal and the vibration level is significantly increased. On the contrary, for 3D vortex shedding, the vortex-induced vibration level is reduced.

For the rough leading edge, Figure 4 right, and in comparison with the smooth configuration, the overall vibration level is increased as well as the vortices span-wise organization. In this time window, the cavitation vortices exhibit essentially 2D pattern. This a fundamental change in the vortices generation process compare to the one with the smooth leading edge. For the latest, the cavitation vortices exhibit essentially 3D pattern. Only rarely, the 2D pattern is evidenced and the vibration amplitude increased. As a result for the rough configuration, the vibration amplitude is higher in comparison with the smooth case.

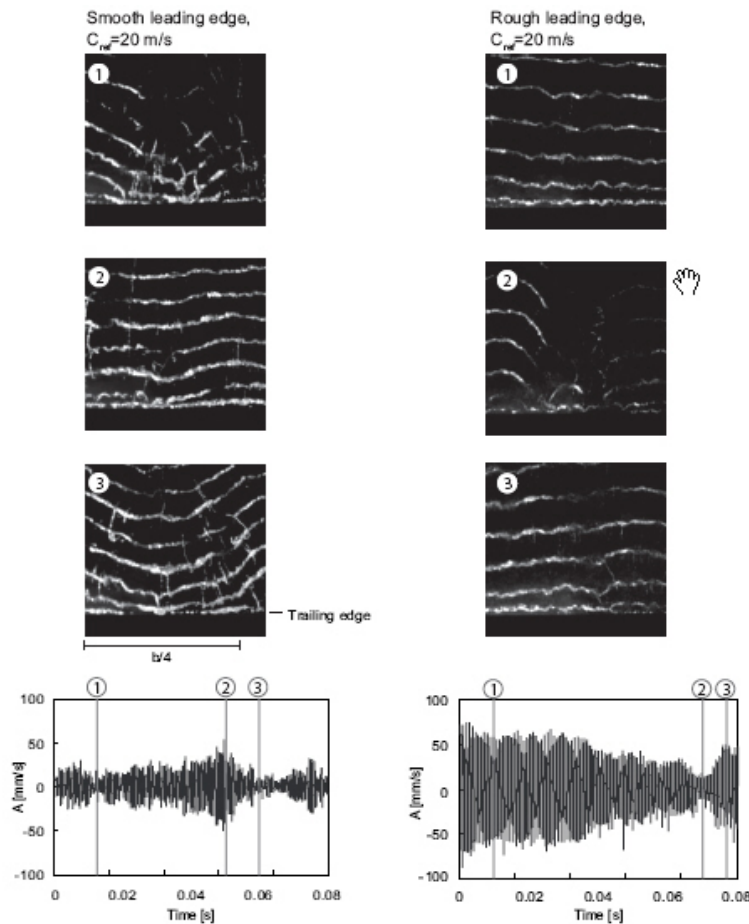


Figure 4. Top-view visualization of cavitation von Kármán vortex street and vortex-induced vibration signal and spectrum for lock-off condition: (Left) Smooth leading edge, (Right) Rough leading edge

4. DISCUSSION AND CONCLUSION

The wake structures visualization has revealed that the span-wise organization is significantly enhanced with the triggered transition to turbulence. As a result, the vortex-induced vibration is increased. The modulation of the vibration signal is next considered: A waterfall spectra of the vibration envelope signals is presented in Figure 5 smooth leading edge. The envelope spectra reveal energy at low frequency but without any characteristic frequency. As a result, the occurrence of the weak shedding cycles, which correspond to vortex dislocations, is non-periodic. Nevertheless, Figure 4 reveals that the time signal for the natural transition is more intermittent than the one for the triggered transition.

Obviously, the shedding process of the von Kármán vortices is highly related to the state of the boundary layer over the entire hydrofoil. In the case of natural laminar-turbulent transition, it is believed that the non-uniform spanwise turbulence development in the boundary layer lead to slight instantaneous variation in vortex shedding frequency along the span which is enough to trigger vortex dislocations, accordingly to the description of the “natural vortex dislocations”, Williamson². On the other hand, for the roughened leading edge, the location of turbulent transition is triggered which reduces the span-wise non uniformities in the boundary layer transition process. The span-wise organization of the von Kármán vortices is enhanced and the vortex-induced vibration level is increased.

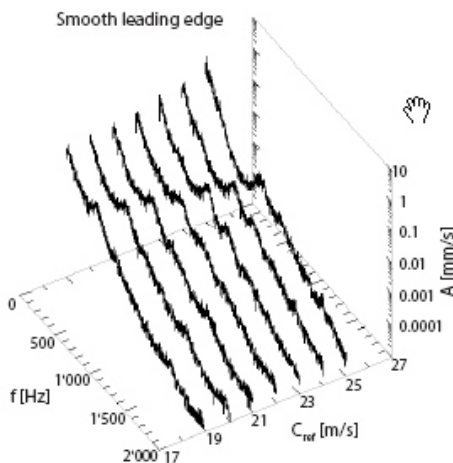


Figure 5 : Waterfall spectra of the vibration envelope signal for lock-off conditions

ACKNOWLEDGMENTS

The investigation reported in this paper is part of the work carried out for the HYDRODYNA, Eureka Research Project n° 3246, whose partners are ALSTOM Hydro, EDF-CIH, EPFL, GE Hydro, UPC-CDIF, VATECH Hydro and VOITH-SIEMENS Hydro Power Generation. The project is also financially supported by

CTI the Swiss Federal Commission for Technology and Innovation grant n° 7045-1 and NSF the Swiss National Science Foundation grant n° 2000-068320. The authors are very grateful to the HYDRODYNA Technical Committee for its involvement and constant support to the project. Finally the staff of the EPFL Laboratory for Hydraulic Machines should be thanked for its support in the experimental and numerical work.

REFERENCES

1. C.H.K. Williamson, “Vortex dynamics in the cylinder wake”, *Annu. Rev. Fluid Mech.*, 28:477-539 (1996)
2. C.H.K. Williamson, “The natural and forced formation of spot-like vortex dislocations in the transition of a wake”, *J.Fluid Mech.*, 243:393-441 (1992)
3. S. Szepessy, “On the spanwise correlation of vortex shedding from a circular cylinder at high subcritical Reynolds number”, *Phys. Fluids* 6(7):2406-2416 (1994)
4. E. Achenbach, E. Heinecke, “On vortex shedding from smooth and rough cylinders in the range of Reynolds numbers 6×10^3 to 5×10^5 ”, *J. Fluid Mech.*, 109: 239-251 (1981)
5. J.C.K. Cheung, W.H. Melbourne., “Turbulence effects on some aerodynamic parameters of a circular cylinder at supercritical Reynolds numbers”, *J. Wind Engng Ind. Aero.*, 14:399-410 (1983)
6. H.M. Blackburn, W.H. Melbourne, “The effect of free-stream turbulence on sectional lift forces on a circular cylinder”, *J. Fluid Mech.*, 306:267-292 (1996)
7. Ph. Ausoni, M. Farhat, Y. Ait Bouziad, J.L. Kueny, F. Avellan, “Kármán vortex shedding from a 2D hydrofoil: Measurement and numerical validation”, *Proc. IAHR Int. Meeting of WG on Cavitation and Dynamic Problems in Hydraulic Machinery and Systems*, Barcelona, Spain, (2006)
8. J. Young, J. Holl, “Effects of cavitation on periodic wakes behind symmetric wedges”, *J. Basic Engrg*”, 88:163-176 (1966)
9. Ph. Ausoni, M. Farhat, X. Escaler, F. Avellan, “Cavitation in Kármán vortices and flow induced vibrations”, *Proc. Sixth International Symposium on Cavitation*, Wageningen, The Netherlands (2006)
10. Ph. Ausoni, M. Farhat, X. Escaler, E. Egusquiza, F. Avellan, “Cavitation influence on Kármán vortex shedding and induced hydrofoil vibrations”, *J.Fluids Eng.*, 129: 966-973 (2007)
11. F. Avellan, P. Henry, I. Ryhming, “A new high speed cavitation tunnel”, *ASME Winter Annual Meeting*, Boston (USA), 57: 49-60 (1987)
12. J.F. Caron, M. Farhat, F. Avellan, “On the leading edge cavity development of an oscillating hydrofoil”, *ASME Fluids Engineering Division Summer Meeting*, Boston (USA), FEDSM2000-11016 (2000)
13. Y. Ait Bouziad, “Physical modelling of the leading edge cavitation: Computational methodologies and application to hydraulic machinery”, PhD thesis, EPFL, N0 3353 (2005)
14. H.L. Dryden, “Review of published data on the effect of roughness on transition from laminar to turbulent flow”, *J. Aeronautical Science*, 20: 477-482 (1953)
15. S. Szepessy, P.W. Bearman, “Aspect ratio and end plate effects on vortex shedding from a circular cylinder”, *J.Fluid Mech.*, 234:191-217 (1992)